

## Redox Properties of Flavocytochrome $c_3$ from *Shewanella frigidimarina* NCIMB400<sup>†</sup>

K. L. Turner,<sup>‡</sup> M. K. Doherty,<sup>§</sup> H. A. Heering,<sup>‡</sup> F. A. Armstrong,<sup>§</sup> G. A. Reid,<sup>||</sup> and S. K. Chapman<sup>\*,‡</sup>

Department of Chemistry, University of Edinburgh, The King's Buildings, West Mains Road, Edinburgh EH9 3JJ, Scotland, Department of Chemistry (Inorganic Chemistry Laboratory), Oxford University, Oxford OX1 3QR, England, and Institute of Cell and Molecular Biology, University of Edinburgh, Mayfield Road, Edinburgh EH9 3JR, Scotland

Received November 4, 1998; Revised Manuscript Received January 8, 1999

**ABSTRACT:** The thermodynamic and catalytic properties of flavocytochrome  $c_3$  from *Shewanella frigidimarina* have been studied using a combination of protein film voltammetry and solution methods. As measured by solution kinetics, maximum catalytic efficiencies for fumarate reduction ( $k_{\text{cat}}/K_m = 2.1 \times 10^7 \text{ M}^{-1} \text{ s}^{-1}$  at pH 7.2) and succinate oxidation ( $k_{\text{cat}}/K_m = 933 \text{ M}^{-1} \text{ s}^{-1}$  at pH 8.5) confirm that flavocytochrome  $c_3$  is a unidirectional fumarate reductase. Very similar catalytic properties are observed for the enzyme adsorbed to monolayer coverage at a pyrolytic graphite "edge" electrode, thus confirming the validity of the electrochemical method for providing complementary information. In the absence of fumarate, the adsorbed enzyme displays a complex envelope of reversible redox signals which can be deconvoluted to yield the contributions from each active site. Importantly, the envelope is dominated by the two-electron signal due to FAD [ $E^\circ = -152 \text{ mV}$  vs the standard hydrogen electrode (SHE) at pH 7.0 and 24 °C] which enables quantitative examination of this center, the visible spectrum of which is otherwise masked by the intense absorption bands due to the hemes. The FAD behaves as a cooperative two-electron center with a pH-dependent reduction potential that is modulated ( $\text{p}K_{\text{ox}}$  at 6.5) by ionization of a nearby residue. In conjunction with the kinetic  $\text{p}K_a$  values determined for the forward and reverse reactions (7.4 and 8.6, respectively), a mechanism for fumarate reduction, incorporating His365 and an anionic form of reduced FAD, is proposed. The reduction potentials of the four heme groups, estimated by analysis of the underlying envelope, are  $-102$ ,  $-146$ ,  $-196$ , and  $-238 \text{ mV}$  versus the SHE at pH 7.0 and 24 °C and are comparable to those determined by redox potentiometry.

Flavocytochrome  $c_3$  is a unique fumarate reductase ( $M_r = 63.8 \text{ kDa}$ ) isolated from the marine bacterium *Shewanella frigidimarina* NCIMB400 (1) formerly known as *Shewanella putrefaciens*. The bacterium itself is unusual in that it is capable of respiration with a wide variety of terminal electron acceptors, including nitrate, nitrite, TMAO, Fe(III), Mn(III), Mn(IV), and fumarate. It is this capability that has implicated the organism in the corrosion of deep sea piping and the spoilage of food (2–4). Production of flavocytochrome  $c_3$  is induced, under anaerobic growth conditions, by the addition of fumarate (5, 6).

The FAD-containing active site regions of several fumarate reductases, including those from *Escherichia coli* (7) and *Wolinella succinogenes* (8), are conserved in flavocytochrome  $c_3$ . However, flavocytochrome  $c_3$  differs from these enzymes in that it is periplasmic and soluble, and there are major structural differences. Fumarate reductase (FRD) from *E. coli* is a membrane-bound enzyme which consists of four

subunits. Subunit A contains a covalently bound FAD, while subunit B contains three iron–sulfur clusters; together, these comprise a membrane extrinsic domain (FrdAB). Two further subunits, C and D, act as membrane anchors (9). FrdAB can be prepared as a soluble subcomplex capable of catalyzing fumarate reduction by small electron donors. The fumarate reductase from *W. succinogenes* is bound to the membrane by a single subunit that contains two *b*-type heme groups (8). In contrast, flavocytochrome  $c_3$  is a single-subunit protein composed of two domains. The active site of the enzyme is located in the flavin domain (454 amino acid residues) which contains noncovalently bound FAD (5). The cytochrome domain (117 amino acid residues), located at the N-terminus of the protein, encapsulates four *c*-type hemes, each of which has bis-His axial ligation. It has been proposed that this domain is structurally similar to the family of cytochrome  $c_3$  proteins such as that from *Desulfovibrio desulfuricans* (10).

Previous redox characterization of flavocytochrome  $c_3$  employed UV–visible-monitored potentiometry, and results indicated that the heme groups might function as two pairs (11). However, the determination of the redox properties of the flavin by this method was not feasible since its absorption spectrum is obscured by intense transitions from the four hemes. In view of the central importance of the FAD in catalysis, we have undertaken a study of the enzyme by

<sup>†</sup> K.L.T. and M.K.D. acknowledge studentships from the BBSRC. H.A.H. and F.A.A. were supported by a grant from the Wellcome Trust (042109). This work was supported by the BBSRC, Zeneca Life Science Molecules, and the Leverhulme Trust.

\* To whom correspondence should be addressed. Fax: 00-44-131-650-4760. E-mail: skc01@holymood.ed.ac.uk.

<sup>‡</sup> Department of Chemistry, University of Edinburgh.

<sup>§</sup> Oxford University.

<sup>||</sup> Institute of Cell and Molecular Biology, University of Edinburgh.

protein film voltammetry (PFV). This technique involves the voltammetric investigation of proteins that are immobilized in a highly electroactive state on an electrode surface, such that their native catalytic properties are retained (12, 13). With such a configuration, both thermodynamic and kinetic properties of redox centers can be studied simultaneously, and information is obtained in both potential and time domains. PFV has been important in studying other multi-centered redox enzymes that catalyze fumarate reduction, e.g., the soluble component of *E. coli* fumarate reductase and succinate dehydrogenase from bovine heart mitochondria (14–19).

In this paper, we show that PFV enables for the first time the observation of all five redox centers in flavocytochrome  $c_3$ , over a wide range of pH values. The FAD is uniquely distinguished by this technique, while the reduction potentials of the four heme groups (which are resolved from a broad envelope) agree well with the results from independent potentiometric titrations. The electrochemical data complement kinetic studies and account for the catalytic bias toward fumarate reduction (vs succinate oxidation) and the pH dependence of activities.

## MATERIALS AND METHODS

**Protein Purification.** Flavocytochrome  $c_3$  from *S. frigidimarina* NCIMB400 was purified as described previously by Pealing et al. (10). Samples for PFV were subjected to an additional purification step using FPLC (fast protein liquid chromatography; Pharmacia) with a Mono Q column [equilibration buffer (pH 7.8) is 10 mM HEPES [*N*-(2-hydroxyethyl)piperazine-*N'*-2-ethanesulfonic acid]; high-salt buffer is 1 M NaCl in equilibration buffer]. The pHs of buffers were adjusted at 20 °C by addition of NaOH. Protein concentrations were determined using the Soret band extinction coefficient of the reduced enzyme ( $752.8 \text{ mM}^{-1} \text{ cm}^{-1}$  at 419 nm) (10).

**Protein Film Voltammetry.** Electrochemical studies were performed with a mixed buffer system of 50 mM TAPS [3-[[tris(hydroxymethyl)methyl]amino]propanesulfonic acid], HEPES, MES (4-morpholineethanesulfonic acid), PIPES (1,4-piperazinediethanesulfonic acid), and an additional supporting electrolyte of 0.1 M NaCl. All buffers were titrated to the required pH with NaOH or HCl at 25 °C. Polymyxin B sulfate (Sigma), which stabilizes the adsorbed enzyme by coadsorption, was prepared as a 30 mg/mL stock solution with its pH adjusted to 7.0. The pH values of final solutions were checked at the experimental temperatures.

The thermostated electrochemical cell (15) was housed in a Faraday cage contained within an anaerobic glovebox (vacuum atmospheres) supplied with a nitrogen atmosphere and maintaining the  $\text{O}_2$  level of <2 ppm. The three-electrode system consisted of a pyrolytic graphite “edge” (PGE) rotating disk working electrode (geometrical area of  $0.03 \text{ cm}^2$ ) used in conjunction with an EG&G M636 electrode rotator and control unit, a platinum gauze counter electrode, and, as a reference, a saturated calomel electrode (SCE) held in a Luggin sidearm containing 0.1 M NaCl. Voltammetry was performed with an Autolab electrochemical analyzer (Eco Chemie, Utrecht, The Netherlands) controlled by GPES software and equipped with an analogue Scan Generator and an Electrochemical Detection (increased sensitivity) module.

All potentials given are with reference to the standard hydrogen electrode (SHE); our values are based on an  $E'^{\circ}$ - (SCE) of 241 mV at 25 °C (20).

For each experiment, the working electrode was polished with an aqueous slurry of  $1.0 \mu\text{M}$  alumina (Buehler micropolish) and sonicated thoroughly. Aliquots of enzyme and polymyxin were added to the electrolyte to give final concentrations of  $0.4 \mu\text{M}$  flavocytochrome  $c_3$  and  $200 \mu\text{g L}^{-1}$  polymyxin. Film formation was initiated at 4 °C, with the electrode rotating at 200 rpm and with a fixed potential of 240 mV for 30 s. The extent of formation was then monitored by cycling at  $100 \text{ mV s}^{-1}$  over the range of 240 to –640 mV until no further development of the signal was observed. This process typically took 7 min, after which cyclic voltammograms were recorded at either 4 or 24 °C without moving the electrode to a different cell. Cyclic voltammograms were obtained at 24 °C by rapid reequilibration of the same electrode/cell system through its reconnection to a second thermostat external to the glovebox. The higher temperature was used to obtain reduction potentials and higher activity catalytic data that could be compared directly with the potentiometric and steady-state solution measurements. The nonturnover voltammograms obtained in this way were corrected for background current using a cubic splines interpolation with fast Fourier transform smoothing (16).

The fumarate reductase activity of the adsorbed flavocytochrome  $c_3$  was studied over a range of fumarate concentrations at 24 °C and pH 7.0. A fresh film, for which the electroactive coverage was measured, was prepared for each fumarate concentration. The electroactive enzyme concentration at the electrode surface (the “electroactive coverage”) was determined by integration of the nonturnover signals (see below). On addition of the required level of fumarate (ICN Chemicals), the limiting current was recorded at –640 mV for several rotation rates (2500–450 rpm) first in order of decreasing rotation rate and then repeated in increasing order. The average of the two values for each rotation rate was used. Following data acquisitions, fresh substrate-free electrolyte was introduced into the cell and the coverage was remeasured. The maximal fumarate reductase activity of the immobilized enzyme was measured at four pH values. Fresh enzyme films were prepared, and fumarate was added to give a concentration of  $200 \mu\text{M}$  (several-fold higher than the  $K_m$ ). The maximum current (2500 rpm) at –640 mV was measured in each case.

**Potentiometric Titrations.** Redox titrations were conducted within a Belle Technology glovebox under a nitrogen atmosphere, with the  $\text{O}_2$  level maintained at less than 6 ppm. A  $10 \mu\text{M}$  flavocytochrome  $c_3$  solution was made up in 0.1 M phosphate buffer (10 mL, pH 7.0), and soluble mediators ( $10$ – $20 \mu\text{M}$  each) of anthraquinone-2-sulfonate, benzyl viologen, methyl viologen, FMN, phenazine methosulfate, and 2-hydroxy-2,4-naphthoquinone were added. The solution was titrated electrochemically according to the method of Dutton (21) using sodium dithionite (BDH) as a reductant and potassium ferricyanide (Analar) as an oxidant. After each reductive/oxidative addition, 10–15 min of equilibration time was allowed. Spectra were recorded on a Shimadzu 1201 UV–vis spectrophotometer (between 800 and 450 nm) contained within the anaerobic environment. The electrochemical potential of the sample solutions was monitored

using a CD740 meter (WPA) coupled to a Pt/calomel electrode (Russell pH Ltd.) at  $25 \pm 2^\circ\text{C}$ . The electrode was calibrated using the  $\text{Fe}^{\text{III}}/\text{Fe}^{\text{II}}$  EDTA couple as a standard (108 mV vs the SHE), and all values are reported versus the standard hydrogen electrode.

**Kinetic Analysis.** The steady-state kinetics of fumarate reduction over a range of pH values were determined using an adaptation of the technique described by Thorneley (22). All experiments were carried out with a Shimadzu UV-PC 1201 spectrophotometer contained in a Belle Technology glovebox at  $25^\circ\text{C}$ . The fumarate-dependent reoxidation of reduced methyl viologen was monitored at 600 nm. The assay buffer contained 0.45 M NaCl, 0.05 M HCl, and 0.2 M methyl viologen (Aldrich) and was adjusted to the required pH using Trizma base (pH range of 7–9). The viologen was reduced by addition of sodium dithionite until an absorbance reading of  $\sim 1$  was obtained. Fumarate was added to give a range of concentrations (0–350  $\mu\text{M}$ ), and the reaction was initiated by addition of the enzyme to a concentration of 0.5  $\mu\text{M}$ . Assays at pH values below 7 or above 8.5 were prepared with standard buffer systems: MES/NaOH (pH 5.4–6.8), CHES/NaOH [2-(*N*-cyclohexylamino)-1-propanesulfonic acid, pH 8.6–10], and CAPS/NaOH (3-cyclohexyl-1-propanesulfonic acid, pH 9.7–11.1).

The ability of flavocytochrome  $c_3$  to act as a succinate dehydrogenase was determined over a range of pH values. All experiments were carried out with a Shimadzu UV-PC 1601 spectrophotometer under aerobic conditions, at  $25^\circ\text{C}$ . Assay buffers were prepared like they were for fumarate reductase assays but using dichloroindophenol (Sigma) as the electron acceptor. This was prepared as a 4 mM stock with 0.27 mM phenazine methosulfate and then added to give a final concentration of 40  $\mu\text{M}$ . Succinate (Aldrich) was added to give a range of concentrations (0–10 mM), and the reaction was monitored at 600 nm after addition of flavocytochrome  $c_3$ . The extent of variation of the maximal rate with pH was determined by carrying out the above assays at concentrations of substrate well in excess of saturating conditions (6 mM fumarate or 8 mM succinate).

## RESULTS

**Flavocytochrome  $c_3$  Voltammograms.** Films prepared on a PGE using highly purified flavocytochrome  $c_3$  with polymyxin B as a coadsorbate showed high electroactivity, fumarate reductase activity, and stability. Rotating the electrode in a dilute solution of enzyme at  $4^\circ\text{C}$  causes the formation of characteristic nonturnover cyclic voltammetric signals, in the form of a broad envelope of oxidation and reduction peaks, which are insensitive to the electrode rotation rate and thus arise from a nondiffusing redox system. Films prepared without polymyxin showed lower-intensity signals which were less stable. The ability of the polymyxin promoter to improve the interaction of the enzyme with the electrode may exist because of the creation of ternary salt bridges between the two surfaces (12). On addition of fumarate, the envelope of signals transforms into a catalytic wave, which is peak-like at a stationary electrode, but becomes sigmoidal and grows in size as the electrode is rotated at increasing speeds (Figure 1). The fumarate reductase activity of the immobilized enzyme was determined quantitatively after rapid re-equilibration at  $24^\circ\text{C}$ . The

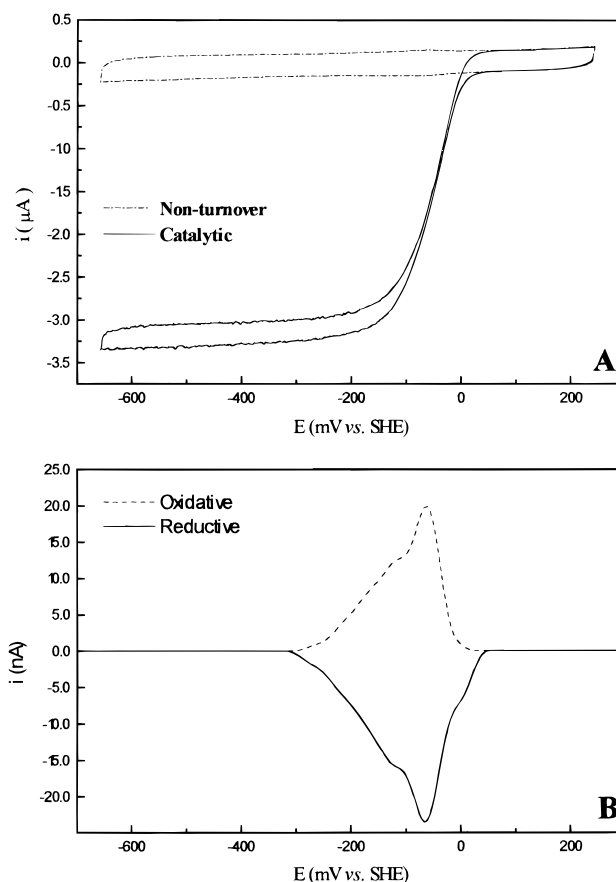


FIGURE 1: (A) Conversion of nonturnover cyclic voltammograms to catalytic sigmoidal waveforms on addition of fumarate. (B) Baseline-corrected nonturnover signals under the same conditions (20  $\text{mV s}^{-1}$ , pH 5, and  $4^\circ\text{C}$ ).

catalytic current was measured at an electrode potential  $E$  of  $-624$  mV for different rotation rates and fumarate concentrations, and the data were analyzed as described previously using Koutecky–Levich (rotation rate dependence) and Michaelis–Menten (substrate concentration dependence of limiting currents obtained from Koutecky–Levich) analyses (15, 16). After the values were normalized with respect to the electroactive surface concentration (see below), the following kinetic parameters resulted:  $k_{\text{cat}} = 1070 \pm 160 \text{ s}^{-1}$ ,  $K_m = 66 \pm 24 \mu\text{M}$ , and thus  $k_{\text{cat}}/K_m = 1.62 \times 10^7 \text{ M}^{-1} \text{ s}^{-1}$ . Degradation of the enzyme films, as measured by the appearance of a free flavin peak at ca.  $-210$  mV (pH 7) or by a decrease in the catalytic current, was minimal at pH 7.0, with the greatest instability being observed at the most extreme pH values used, pH 5 and 9.

**Thermodynamics of the Electron-Transfer Pathway at pH 7 and  $24^\circ\text{C}$ .** The baseline-corrected nonturnover voltammograms represent the reversible electrochemistry of five redox centers. As shown in Figure 2, the most prominent feature is a sharp signal that shifts to more negative potentials at higher pH values, and which is assigned to the two-electron redox couple of the FAD. This signal dominates a broader envelope containing the overlapping contributions of the four one-electron heme centers. At low pH values, two additional features were often evident. One signal, consisting of an oxidation and reduction peak with a reduction potential ca. 80 mV more negative than the signal due to enzyme-bound flavin, appeared as a result of flavin dissociation despite film preparation occurring at low temperatures. The other feature



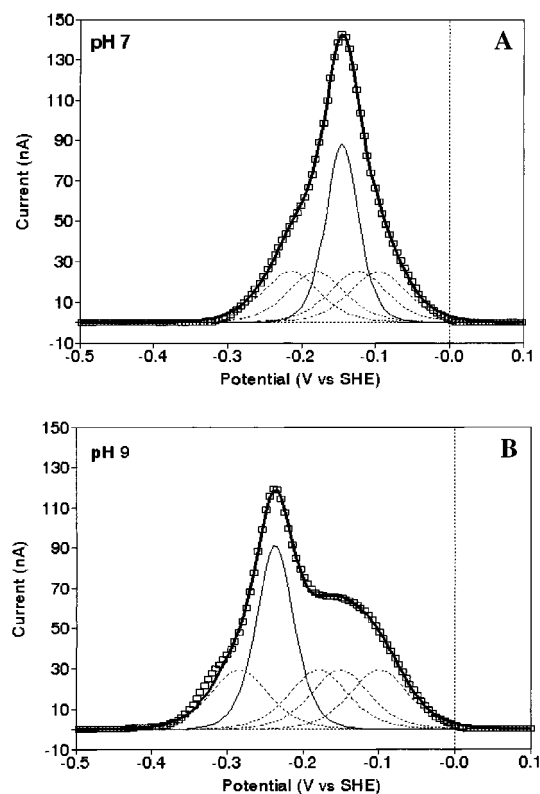


FIGURE 2: Baseline-corrected nonturnover oxidative scan at (A) pH 7.0 and (B) pH 8.8 (24 °C): smoothed data ( $\square$ ) and deconvoluted data for fit ( $\blacksquare$ ), flavin (—), and hemes (---).

was a small “shoulder” which appeared only in the positive potential flank of the reductive scan. This represented a low but variable contribution as compared to the rest of the broad envelope, raising the interesting possibility that this is a catalytic current due to contamination from trace levels of substrate. Indeed, the enzyme activity is sufficiently high, particularly at this pH, that even nanomolar levels of fumarate should produce observable reduction currents in this region of potential (19). Consequently, under low-pH conditions, data from the two potential extremes of the envelope were excluded from the fitting procedure.

Deconvolution of the nonturnover peaks was performed by a least-squares fit to the sum of the five voltammetric peaks with equal surface concentrations. The shape of each peak is described by eq 1 (23).

$$i = \frac{n_s n_{\text{app}} F^2 \nu A \Gamma}{RT} \frac{\exp[n_{\text{app}} F(E - E_p)/RT]}{[1 + \exp[n_{\text{app}} F(E - E_p)/RT]]^2} \quad (1)$$

where  $\nu$  is the scan rate (volts per second),  $\Gamma$  is the surface concentration (moles per square centimeter),  $A$  is the electrode area (square centimeter),  $E$  is the applied potential (volts),  $E_p$  is the potential at the peak maximum (volts),  $n_s$  is the stoichiometric number of electrons, and  $n_{\text{app}}$  is the apparent number of electrons as determined from the peak width at half-height,  $\delta$ , where

$$\delta = 3.53 \frac{RT}{n_{\text{app}} F} \quad (1A)$$

The four heme signals were assumed to be ideal one-electron peaks ( $n_{\text{app}} = n_s = 1$ ). The FAD was treated as a two-electron

Table 1: Comparison of the Formal Reduction Potentials (Millivolts vs the SHE) Determined from Reductive and Oxidative Titrations of Flavocytochrome  $c_3$  during Solution and the Noncatalytic Cyclic Voltammetry of the Enzyme Film at pH 7.0<sup>a</sup>

potential	oxidative titration <sup>b</sup>	reductive titration <sup>b</sup>	voltammetry <sup>b</sup>	voltammetry <sup>c</sup>
$E_{\text{FAD}}$	ND	ND	$-152 \pm 2$	$-125 \pm 2$
$E_1$	$-80 \pm 15$	$-96 \pm 15$	$-102 \pm 20$	$-94 \pm 10$
$E_2$	$-142 \pm 15$	$-163 \pm 15$	$-146 \pm 10$	$-140 \pm 15$
$E_3$	$-195 \pm 15$	$-223 \pm 15$	$-196 \pm 10$	$-170 \pm 15$
$E_4$	$-274 \pm 15$	$-280 \pm 15$	$-238 \pm 20$	$-224 \pm 10$

<sup>a</sup>  $E_{\text{FAD}}$  is the potential of the two-electron reduction of the FAD group, and  $E_1$ – $E_4$  are the potentials of the four successive one-electron reductions of the tetra-heme moiety. <sup>b</sup> At 25 °C. <sup>c</sup> At 4 °C.

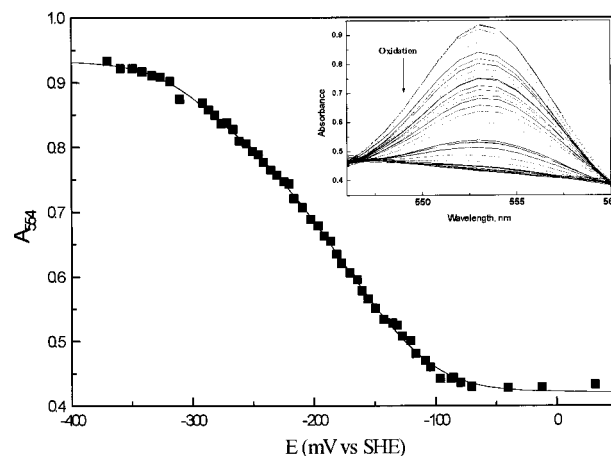


FIGURE 3: Oxidative titration of flavocytochrome  $c_3$  with ferricyanide (pH 7 and 25 °C). The inset shows successive spectra monitoring the extent of heme oxidation. The main graph shows the plot of the extent of heme reduction, measured at  $\text{Abs}_{554}$ , as a function of the reduction potential ( $\circ$ ), and the best fit of the data ( $\blacksquare$ ) to eq 2, yielding the following estimates:  $E_1 = -80$  mV vs the SHE,  $E_2 = -142$  mV vs the SHE,  $E_3 = -195$  mV vs the SHE, and  $E_4 = -274$  mV vs the SHE.

peak ( $n_s = 2$ ) where the parameter of  $n_{\text{app}}$  was fitted to give an indication of the degree of cooperativity between the two one-electron reduction steps of the flavin (see the Discussion). Two extra parameters for an additional linear baseline correction resulted in a nine-parameter fit. Deconvolution revealed that the total contribution from four independent heme centers is double that of the FAD, i.e., as expected if all these groups are electroactive. Attempts to decrease the contributions of the one-electron centers relative to that of the sharp FAD component gave less satisfactory fits. Electroactive coverages (based upon six-electron capacity) were quite uniform over the pH range of 5–9 (approximately  $9 \times 10^{-12}$  mol  $\text{cm}^{-2}$ ), and the average value of  $n_{\text{app}}$  for FAD was  $1.60 \pm 0.12$ , which again showed little variation with pH. The estimated reduction potentials at pH 7.0 and 24 °C are listed in Table 1.

The reduction potentials of the four hemes of flavocytochrome  $c_3$  were also investigated by potentiometric titrations. Results are shown in Figure 3. The degree of heme reduction was monitored in both the reductive and oxidative directions using the change ( $\Sigma\text{Abs}$ ) in the heme UV–vis absorbance at 554 nm, and was fully reversible. At this wavelength, there is negligible absorbance change due to the FAD. The absorbance change due to methyl viologen only contributed significantly at potentials below  $-350$  mV when reduction

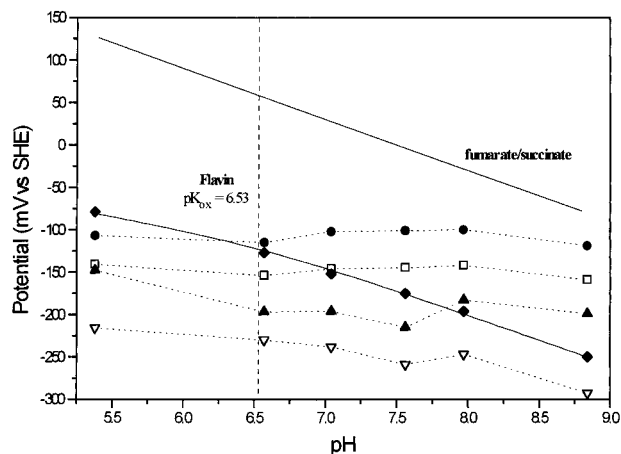


FIGURE 4: pH dependence of the midpoint potentials of all five redox centers at 24 °C, determined by voltammetry of flavocytochrome  $c_3$  films [hemes (●, □, ▲, and ▼) and flavin (◆)]. The solid line represents the pH dependence of the fumarate/succinate redox couple (30 mV, pH 7, and 25 °C) (24).

of the enzyme was already complete. Absorbance data were the convoluted results for the complete reduction of the tetra-heme moiety, which has five different net redox states. The experimental data were fitted to a model, described by eq 2, in which each one-electron reduction ( $i = 1-4$ ) causes a quarter of the total absorbance change.

$$\sum \text{Abs} = \sum_{i=1}^4 \frac{\epsilon_{\text{ox}} + \epsilon_{\text{red}} \exp\left[\frac{F(E_i - E)}{RT}\right]}{1 + \exp\left[\frac{F(E_i - E)}{RT}\right]} \quad (2)$$

The absorption coefficients  $\epsilon_{\text{ox}}$  and  $\epsilon_{\text{red}}$  are for one oxidized and one reduced heme, respectively;  $E$  is the applied potential (millivolts), and  $E_i$  is the formal reduction potential with initial estimates taken from the PFV data. In Table 1, the parameters derived for the reductive and oxidative titrations are compared with the cyclic voltammetry data. There was no evidence for any cooperativity between the heme groups, and the data obtained from both techniques showed good fits with the proposed model of four independent hemes.

**pH Studies of the Thermodynamics of the Electron-Transfer Pathway.** Figure 4 shows the pH dependence of reduction potentials determined by deconvolution of non-turnover cyclic voltammograms at 24 °C. The reduction potential of the flavin signal shows a significant dependence on pH. Flavin reduction at low pH is accompanied by the transfer of one proton (limiting slope of 30 mV/pH unit), but at higher pH values, two protons are transferred (limiting slope of 60 mV/pH unit). The two-electron FAD potentials were fitted to a model for two-electron flavin reduction which is dependent on the protonation status of one site (eq 3)

$$E_{\text{FAD}} = E_0 + \frac{RT}{2F} \ln\left(\frac{[\text{H}^+]^2}{[\text{H}^+] + K_{\text{ox}}}\right) \quad (3)$$

where  $[\text{H}^+]$  is  $10^{-\text{pH}}$ ,  $K_{\text{ox}}$  is the equilibrium constant for the (de)protonation of the site, and  $E_0$  is the hypothetical reduction potential at pH 0 (24).

Table 2: Summary of the Parameters Determined for Fumarate Reduction by Flavocytochrome  $c_3$  at a Range of pH Values<sup>a</sup>

pH	$k_{\text{cat}}$ ( $\text{s}^{-1}$ )	$K_{\text{m}}$ ( $\mu\text{M}$ )	$k_{\text{cat}}/K_{\text{m}}$ ( $\text{M}^{-1} \text{s}^{-1}$ )
6.0	$658 \pm 34$	$43 \pm 10$	$1.5 \times 10^7$
7.0	$587 \pm 40$	$36 \pm 8$	$1.6 \times 10^7$
7.2	$509 \pm 15$	$25 \pm 2$	$2.1 \times 10^7$
7.6	$409 \pm 13$	$29 \pm 3$	$1.4 \times 10^7$
8.0	$345 \pm 20$	$18 \pm 4$	$1.9 \times 10^7$

<sup>a</sup> All data were collected in an anaerobic environment at 25 °C using the solution assay system described in Materials and Methods.

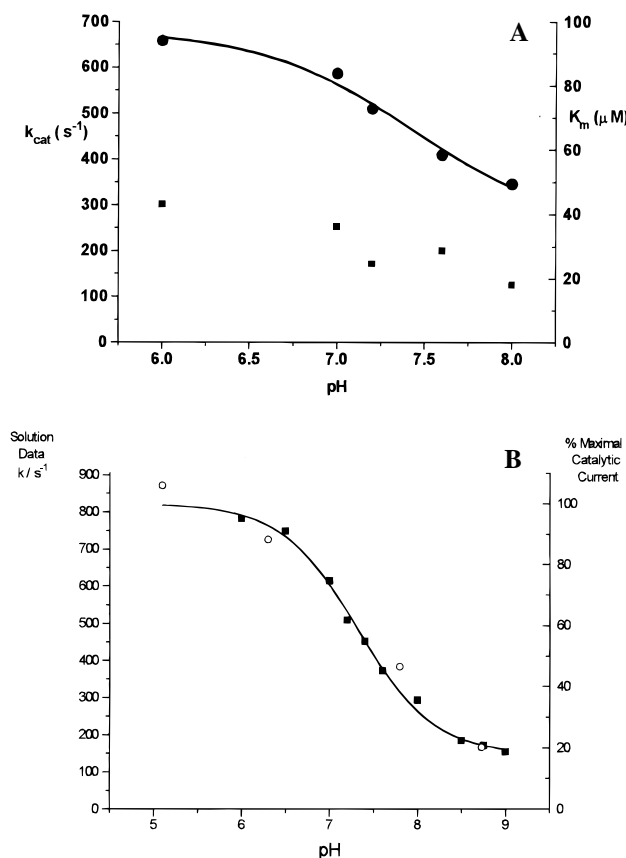


FIGURE 5: (A) Effect of pH on the catalytic parameters of fumarate reduction by flavocytochrome  $c_3$  as determined by anaerobic solution studies carried out at 25 °C.  $k_{\text{cat}}$  data are denoted with ● and  $K_{\text{m}}$  data denoted with ■. (B) pH dependence of fumarate reduction by flavocytochrome  $c_3$  in solution (■) and adsorbed at an electrode (○). The estimated  $\text{pK}_a$  for solution data is  $7.32 \pm 0.04$  (6 mM fumarate).

Estimated values follow:  $\text{pK}_{\text{ox}} (-\log K_{\text{ox}}) = 6.52 \pm 0.14$  and  $E_0 = 78.3 \pm 3.1$  mV at 24 °C (7.12 and 78.0, respectively, at 4 °C). The heme potentials do not show such clear trends as a function of pH; however, they can be grouped into two pairs with the lower potential pair showing a greater dependence on both pH and temperature.

**pH Dependence of the Catalytic Properties of Flavocytochrome  $c_3$ .** Kinetic characterization of flavocytochrome  $c_3$  was carried out over a range of pH values, and the resulting Michaelis–Menten parameters are shown in Table 2. Figure 5A shows how the catalytic parameters  $k_{\text{cat}}$  and  $K_{\text{m}}$  are affected by pH. The turnover number for fumarate reduction increases from  $350 \text{ s}^{-1}$  at pH 8 to almost  $600 \text{ s}^{-1}$  at pH 7. Further analysis of these data yielded a  $\text{pK}_a$  value of  $7.43 \pm 0.16$ . With 6 mM fumarate, the similarity of the pH dependence of  $k_{\text{obs}}$  to that of  $k_{\text{cat}}$  confirmed that this

Table 3: Summary of Kinetic Parameters Determined for Succinate Oxidation by Flavocytochrome  $c_3$ <sup>a</sup>

pH	$k_{\text{cat}}$ (s <sup>-1</sup> )	$K_m$ (mM)	$k_{\text{cat}}/K_m$ (M <sup>-1</sup> s <sup>-1</sup> )
8.0	0.60 ± 0.05	2.2 ± 0.4	272
8.5	0.70 ± 0.02	0.8 ± 0.1	933
8.75	0.40 ± 0.01	0.6 ± 0.1	727
9.0	0.73 ± 0.01	1.1 ± 0.1	675
9.5	1.36 ± 0.05	2.5 ± 0.2	544
10.0	0.95 ± 0.02	2.6 ± 0.2	362

<sup>a</sup> All data were collected at 25 °C using the solution assay described in Materials and Methods.

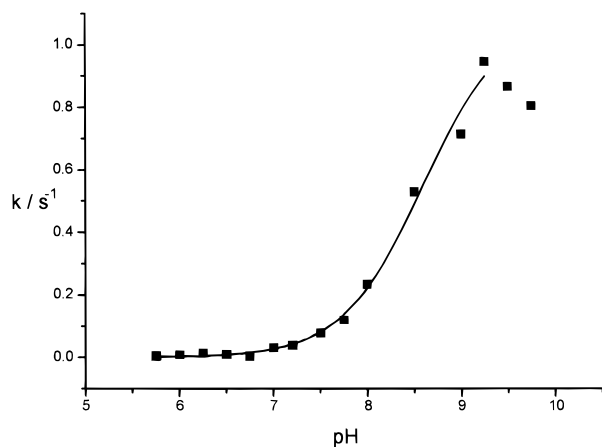


FIGURE 6: Determination of the  $pK_a$  of succinate oxidation by flavocytochrome  $c_3$ . Data were collected at 25 °C under aerobic conditions with 8 mM succinate. Extrapolation of the fitted curve predicts a maximal activity of 1.1 s<sup>-1</sup>.

concentration is essentially saturating, and gave a comparable  $pK_a$  value of  $7.32 \pm 0.10$ . As is evident from Figure 5B, the pH dependence of the fumarate reductase activity of the enzyme is unaltered on immobilization at an electrode, based on the maximum mass-limiting current recorded (200  $\mu\text{M}$  fumarate, 640 mV, 2000 rpm, 24 °C).

It should be noted that there is a similar magnitude of variation for both  $k_{\text{cat}}$  and  $K_m$  over the range of pHs studied. The Michaelis constant,  $K_m$ , does show an overall increase with decreasing pH (a factor of 2 between pH 6 and 8 values), but unlike the pH dependence of  $k_{\text{cat}}$ , it cannot be fitted to a single protonation step.

The reverse reaction, conversion of succinate to fumarate, was also studied, under steady-state conditions, using dichloroindophenol as an oxidant. It was immediately obvious that catalysis in this direction was much slower than for fumarate reduction. Michaelis–Menten parameters were again determined over a range of pH values (8.5–10), and results are given in Table 3. Figure 6 shows the pH dependence of the succinate oxidation activity measured under saturating conditions (8 mM succinate) from which a  $pK_a$  of  $8.59 \pm 0.10$  was determined.

## DISCUSSION

All five redox centers in flavocytochrome  $c_3$  have been investigated by cyclic voltammetry of the enzyme adsorbed as an electroactive monolayer film on a PGE. The thermodynamic and catalytic properties of the enzyme in solution and immobilized at the electrode have been compared. Significantly, the two techniques, with their striking contrasts with regard to the environment imposed on the enzyme, gave

essentially identical catalytic efficiencies for fumarate reduction ( $1.69 \times 10^7$  and  $1.62 \times 10^7 \text{ M}^{-1} \text{ s}^{-1}$  for solution and electrode surface, respectively). The heme reduction potentials are spread over a range of >200 mV, but similar estimates of individual values were obtained by potentiometry (solution) and voltammetry (film) studies. Shifts in potential of ca. 30 mV were observed for the first and last electrons ( $E_1$  and  $E_4$ , respectively) and may indicate the increased difficulty in fitting the one-electron peaks at the edge of the heme envelope. However, the magnitude of this potential shift is consistent with that seen for other proteins on adsorption at an electrode or association with biological components (25) where it has been attributed to slight changes in the environment of a redox center. The perturbation of at least two of the redox centers by the electrode indicates that the orientation of the flavocytochrome  $c_3$  molecule is with the heme domain closest to the electrode surface. Indeed, the high electroactivity alone demands that at least one of the redox centers lies close to the electrode surface. The observation that the flavocytochrome  $c_3$  film exhibits the same thermodynamic and catalytic behavior as the free enzyme in solution confirms that application of film voltammetry to the study of this enzyme is valid. In this case, it is an excellent strategy since the flavin group becomes clearly observable despite the presence of four hemes.

The baseline-corrected nonturnover cyclic voltammograms of flavocytochrome  $c_3$  films were deconvoluted to reveal the signals due to reversible electrochemical response from five redox centers with equal surface concentrations. The typical value of electroactive coverage,  $9 \times 10^{-12} \text{ mol cm}^{-2}$  based on the geometric electrode area, lies between the values of  $7$  and  $17 \times 10^{-12} \text{ mol cm}^{-2}$  expected for a packed monolayer on the basis of different orientations of the enzyme molecule with the following unit cell dimensions:  $a = 77.7 \text{ \AA}$ ,  $b = 86.7 \text{ \AA}$ ,  $c = 211.2 \text{ \AA}$ , and  $V_m = 2.8 \text{ \AA}^3/\text{Da}$  (S. L. Peeling, personal communication). The result is significant, considering our crude assumption of a flat electrode surface. The experimental data are consistent with a model for four independent one-electron hemes and a two-electron flavin. At pH 7.0, the FAD peak width is 56 mV, which for 24 °C is just 11 mV broader than the ideal value for a fully cooperative reaction ( $n_{\text{app}} = n_s = 2$ ) (23). Since dispersion (inhomogeneity) would itself tend to broaden the peak, the result shows that the single electron reduction potential semiquinone/hydroquinone reduction potential,  $E_{\text{sh}}$ , must be at least 29 mV higher than that of the oxidized/semiquinone couple,  $E_{\text{os}}$ ; i.e., the semiquinone state is not stabilized, at least in the substrate-free form of the enzyme (16).

The thermodynamics of the electron-transfer components (pH 7.0 and 25 °C) in flavocytochrome  $c_3$  from *S. frigidimarina* and fumarate reductase from *E. coli* are summarized in Figure 7. The reducing substrate for *E. coli* fumarate reductase is menaquinone ( $E_m = -74 \text{ mV}$ ) (26, 27), whereas the electron donor to flavocytochrome  $c_3$  has not yet been established. In both cases, the electron-transfer mediating groups have reduction potentials which are appropriate for favorable intramolecular electron transfer to their respective flavins; i.e., they are close to or a little lower than  $E_{\text{FAD}}$ . The reduction potential of the fumarate/succinate couple at pH 7.0 is 30 mV (24), and it has been proposed that noncovalently bound FAD, with its lower reduction potential, is unable to mediate efficient succinate oxidation. For the

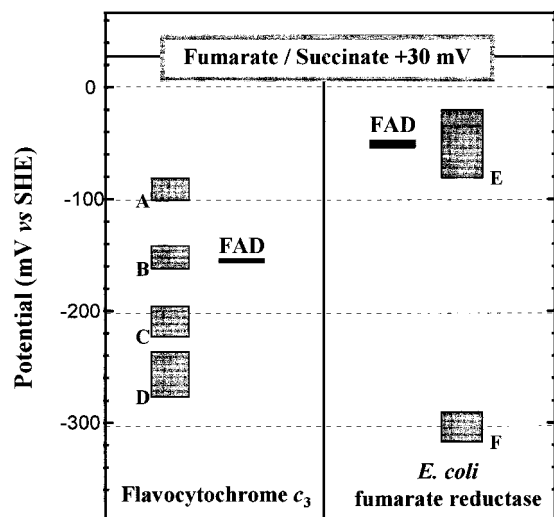


FIGURE 7: Formal reduction potentials of the redox centers in flavocytochrome  $c_3$  (as presented here) and *E. coli* fumarate reductase [several studies, summarized by Heering et al. (16)] at pH 7.0 and 25 °C. A–D are the heme mediating groups in flavocytochrome  $c_3$ ; E and F are the iron–sulfur clusters in *E. coli* fumarate reductase (centers 1 and 3 are E; center 2 is F).

fumarate reductase from *E. coli*, reported values of the reduction potential for the covalently bound FAD are –30 to –55 mV at pH 7.0 (15, 16, 28) [compared to –219 mV for free FAD (29)]. After the conditions of pH have been optimized, this enzyme will catalyze succinate oxidation at 30–40% of the rate at which it reduces fumarate (30). However, replacements of the FAD-binding histidine by serine, arginine, cysteine, or tyrosine produced mutants in which the flavin was bound noncovalently (31). Without the arginine mutant, it was shown that while fumarate reductase activity was only slightly affected, the ability of the enzyme to catalyze succinate oxidation was decreased to 2% of the wild-type capability. Our results now show simultaneously that (a) flavocytochrome  $c_3$  has an extremely low relative activity for succinate oxidation (optimized rates are 3–4 orders of magnitude lower than for fumarate reduction) and (b) the reduction potential  $E_{\text{FAD}}$  (–152 mV at pH 7.0 and 24 °C) is significantly more negative than in the other fumarate reductases, thus upholding the hypothesis for the role of covalent binding in modulating FAD redox activity.

We next consider the effect that pH has on the underlying energetics. Above pH 6.5, the reduction potentials of both the FAD and fumarate have the same pH dependence, i.e., that of a  $2\text{H}^+$ ,  $2\text{e}^-$  transfer (24). The fact that the rate of catalysis of fumarate reduction decreases significantly as the pH is raised therefore suggests that transfer of reducing equivalents from FAD to substrate is not rate-determining. By contrast, and as is evident from Figure 4, increasing the pH causes the FAD to become an increasingly poorer electron acceptor (but better electron donor) relative to the heme groups. The change in energetics is fully consistent with the catalytic trends in either direction; i.e., succinate oxidation rates increase, whereas fumarate reduction is retarded, and strongly implicates intramolecular electron transfer as a decisive factor in the mechanism. This can be kinetic, i.e., transfer of electrons between FAD and hemes possibly being the rate-determining process, or thermodynamic, with redox equilibria being maintained throughout catalysis by fast intramolecular electron transfer.

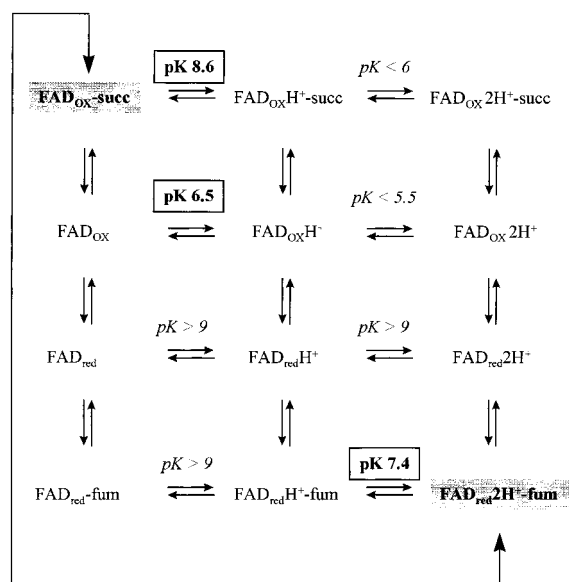


FIGURE 8: Scheme showing the various equilibria involved in the reduction of fumarate by flavocytochrome  $c_3$ . Shaded species show the FAD active site poised to reduce fumarate or oxidize succinate. Vertical steps indicate substrate/product binding and the two-electron flavin reduction. Protonation equilibria and the relevant equilibrium constants are shown horizontally. The measured values are in boxes and the constraints in italics.

Three  $pK$  values are revealed in this study, two kinetic  $pK$  values (7.43 for fumarate reduction and 8.59 for succinate oxidation) and one determined from voltammetry ( $pK_{\text{ox}} = 6.5$ ), which is associated with an ionization close to the oxidized FAD. These measured values have been incorporated into a scheme for the various equilibria involved in the fumarate reduction (Figure 8). An explanation for these ionizations and their roles in the catalytic activity requires consideration of the likely structure of the active site.

It has previously been proposed from sequence comparison studies that the main residues involved in the catalysis of fumarate reduction are Arg381 and Arg554 along with His365 (5). In the suggested mechanism, the two arginine residues were cited as binding sites for the carboxylate groups of fumarate. The histidine, however, was postulated to be the key residue for catalysis. Histidine is commonly found to be an important catalytic residue within this family of enzymes (32). There are also two conserved aspartate residues at positions 197 and 205. Several groups of enzymes, including serine proteases and thermolysin, have been found to contain His-Asp pairs, rather than a single histidine (33). This ion pairing has the effect of shifting the  $pK_a$  of the histidine to around 7.5. In addition, in many flavin-dependent 2- $\alpha$ -hydroxy acid dehydrogenases, the imidazole ring is held in a fixed orientation over the flavin group (34). It has also been noted previously that fumarate reduction and succinate oxidation should show opposite pH dependencies with a single histidine acting as a general acid or base catalyst (35).

A model for the active site of flavocytochrome  $c_3$  which is consistent with the experimental data is shown in Figure 9. Here, the active-site base is His365 and the imidazole ring of this residue is stacked over the flavin group so that their acid–base properties are tightly coupled. Above pH 6.5, addition of two electrons to the FAD is accompanied by the net uptake of two protons, one of which is bound directly to the ring to give an anionic hydroquinone (36) and the other



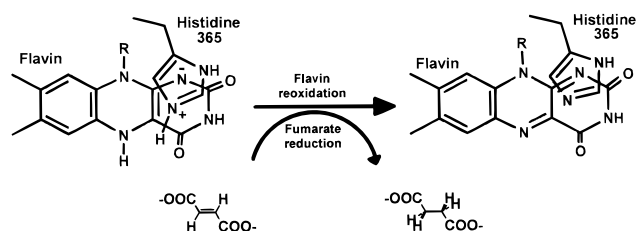


FIGURE 9: Proposed scheme indicating the electroneutrality of the flavin-histidine pair. In the reduced flavin, the anion at N1 is stabilized by an imidazolium ion on His365. Transfer of a hydride ion from flavin N5 and a proton from His365 results in a neutral flavin-histidine pair and the formation of succinate.

to His365. The *pK* of 6.5 can be most easily attributed to protonation of the histidine in the FAD-oxidized state so that two-electron reduction of the FAD below pH 6.5 is accompanied by uptake of just one proton. The ring-stacking arrangement would also ensure the strongly coupled delivery of both a hydride and a proton to fumarate since removal of either one would result in an unstabilized charge.

Confirmation of the role of His365 in both the thermodynamic and catalytic properties of the enzyme is currently under investigation by construction and characterization of a range of mutants. The decrease in fumarate reductase activity on the replacement of the equivalent histidine in *E. coli* fumarate reductase, His232Ser, has already demonstrated the crucial role of this residue in the catalytic cycle (28). The redox characterization of analogous flavocytochrome *c*<sub>3</sub> mutants, in the absence of fumarate reductase activity, will reveal whether protonation of this residue does indeed affect the flavin reduction potential.

In conclusion, we have shown that protein film voltammetry is a useful technique for probing the thermodynamic and kinetic features of flavocytochrome *c*<sub>3</sub> and is particularly important in determining the FAD redox properties which are otherwise obscured. It can clearly be seen that, for this enzyme, results determined with the protein adsorbed onto a solid electrode are comparable to those obtained in the solution phase. A mechanism for the reduction of fumarate, the primary reaction of the enzyme, has been proposed on the basis of the kinetic data presented and is currently under investigation.

## ACKNOWLEDGMENT

K.L.T. is grateful to Kerensa Heffron, Judy Hirst, and Bob Holt (Zeneca Life Science Molecules) for valuable discussions.

## REFERENCES

- Reid, G. A., and Gordon, E. H. J. (1999) *Int. J. Syst. Bacteriol.* 49, 189–191.
- Levin, R. E. (1972) *Antonie van Leeuwenhoek* 38, 121–127.
- Stenstrom, I. M., and Molin, G. (1990) *J. Appl. Bacteriol.* 68, 601–618.
- Dichristina, T. J., and Delong, E. F. (1994) *J. Bacteriol.* 176, 1468–1474.
- Pealing, S. L., Black, A. C., Manson, F. D. C., Ward, F. B., Chapman, S. K., and Reid, G. A. (1992) *Biochemistry* 31, 12132–12140.
- Myers, C. R., and Myers, J. M. (1992) *FEMS Microbiol. Lett.* 98, 13–19.
- Wood, D., Darlison, M. G., Wilde, R. J., and Guest, J. R. (1984) *Biochem. J.* 222, 519–534.
- Kortner, C., Lauterbach, F., Tripiet, D., Unden, G., and Kroger, A. (1990) *Mol. Microbiol.* 4, 855–860.
- Van Hellemond, J., and Tielens, A. G. M. (1994) *Biochem. J.* 304, 321–331.
- Pealing, S. L., Cheeseman, M. R., Reid, G. A., Thomson, A. J., Ward, B., and Chapman, S. K. (1995) *Biochemistry* 34, 6153–6158.
- Morris, C. J., Black, A. C., Pealing, S. L., Manson, F. D. C., Chapman, S. K., Reid, G. A., Gibson, D. M., and Ward, F. B. (1994) *Biochem. J.* 302, 587–593.
- Armstrong, F. A., Heering, H. A., and Hirst, J. (1997) *Chem. Soc. Rev.* 26, 169–179.
- Armstrong, F. A. (1996) in *Bioelectrochemistry and Biomacromolecules* (Lenaz, G., and Milazo, G., Eds.) Chapter 4, pp 205–252, Birkhauser Verlag, Basel, Switzerland.
- Sucheta, A., Ackrell, B. A. C., Cochran, B., and Armstrong, F. A. (1992) *Nature* 356, 362–363.
- Sucheta, A., Cammack, R., Weiner, J., and Armstrong, F. A. (1993) *Biochemistry* 32, 5455–5465.
- Heering, H. A., Weiner, J. H., and Armstrong, F. A. (1997) *J. Am. Chem. Soc.* 119, 11628–11638.
- Hirst, J., Sucheta, A., Ackrell, B. A. C., and Armstrong, F. A. (1996) *J. Am. Chem. Soc.* 118, 5031–5038.
- Hirst, J., Ackrell, B. A. C., and Armstrong, F. A. (1997) *J. Am. Chem. Soc.* 119, 7434–7439.
- Heering, H. A., Hirst, J., and Armstrong, F. A. (1998) *J. Phys. Chem. B* 102, 6889–8902.
- Bard, A. J., and Faulkner, L. R. (1980) *Electrochemical Methods, Fundamentals and Applications*, Wiley, New York.
- Dutton, P. L. (1978) *Methods Enzymol.* 54, 411–435.
- Thorneley, R. N. F. (1974) *Biochim. Biophys. Acta* 333, 487–496.
- Laviron, E. (1982) in *Electroanalytical Chemistry* (Bard, A. J., Ed.) Vol. 12, pp 53–157, Marcel Dekker, New York.
- Clark, W. M. (1960) in *Oxidation-Reduction Potentials of Organic Systems*, pp 125 and 507, Tindall & Cox Ltd., London.
- Willit, J. L., and Bowden, E. F. (1987) *J. Electroanal. Chem.* 221, 265–274.
- Wagner, G. C., Kassner, R. J., and Karmen, M. D. (1974) *Proc. Natl. Acad. Sci. U.S.A.* 71, 253–256.
- Holländer, R. (1976) *FEBS Lett.* 72, 98–100.
- Ackrell, B. A. C., Cochran, B., and Cecchini, G. (1989) *Arch. Biochem. Biophys.* 26, 26–34.
- Lowe, H. J., and Clark, W. M. (1956) *J. Biol. Chem.* 221, 983–992.
- Cecchini, G., Ackrell, B. A. C., Deshler, J. O., and Gunsalus, R. P. (1986) *J. Biol. Chem.* 261, 1808–1814.
- Blaut, M., Whittaker, K., Valdovinos, A., Ackrell, B. A. C., Gunsalus, R. P., and Cecchini, G. (1989) *J. Biol. Chem.* 264, 13599–13604.
- Schroder, I., Gunsalus, R. P., Ackrell, B. A. C., Cochran, B., and Cecchini, G. (1991) *J. Biol. Chem.* 266, 13572–13579.
- Fersht, A. R., and Sperling, J. (1973) *J. Mol. Biol.* 74, 137–149.
- Birktoft, J. J., and Banaszak, L. J. (1983) *J. Biol. Chem.* 258, 472–482.
- Vik, S. B., and Hatefi, Y. (1981) *Proc. Natl. Acad. Sci. U.S.A.* 78, 6749–6753.
- Miles, C. S., Rouvière-Fourmy, N., Lederer, F., Matthews, F. S., Reid, G. A., Black, M. T., and Chapman, S. K. (1992) *Biochem. J.* 285, 187–192.

BI9826308